FISEVIER

Contents lists available at ScienceDirect

Results in Control and Optimization

journal homepage: www.elsevier.com/locate/rico





Mathematical Model for COVID-19 pandemic with implementation of intervention strategies and Cost-Effectiveness Analysis

A. Venkatesh*, M. Ankamma Rao

Department of Mathematics, AVVM Sri Pushpam College (affiliated to Bharathidasan University, India), Poondi, Thanjavur(Dt), Tamilnadu, 613503, India

ARTICLE INFO

Dataset link: https://data.covid19india.org/csv/latest/case time series.csv

Keywords: COVID-19 Sensitivity analysis Vaccine efficacy Vaccine coverage Optimal control problem Cost effectiveness

ABSTRACT

In this study, a novel mathematical model for the dissemination dynamics of COVID-19 is developed. The main objective is to analyze the effectiveness of pharmaceutical interventions in lowering the COVID-19 contagions. We first demonstrate the positivity and boundedness of the solutions of the model and then compute the fundamental reproduction number. The stability analysis of contagion-free equilibrium is performed. The model is fitted to the COVID-19 reported data for a period of twelve months in India and estimate three parameters. The sensitivity analysis is conducted to identify the significant factors which impact the COVID-19 disease prevalence. We then define an optimum control problem using pharmaceutical interventions vaccination and treatment as the control functions to minimize the dissemination of COVID-19 contagions and disease-related mortality. Cost-effectiveness analysis is employed to determine the most effective and least costly strategy. The results are determined that the combination of vaccination and treatment is the most effective and least costly strategy in mitigating the spread of COVID-19 contagions. Furthermore, the impact of different levels of vaccine efficacy on contagion trajectories is examined, and it is shown that COVID-19 contagions and disease related fatalities would decrease as vaccination efficacy increases. The outcomes would assist administrators in developing efficient strategies to reduce the scope of the COVID-19 pandemic.

1. Introduction

Almost all countries in the world have experienced economic damage as a result of the COVID-19 disease. Although various prevention techniques are implemented to slow down the spread of the disease, it is still unclear when this devastating contagion will disappear completely from the population. Currently the majority of countries experience COVID-19 contagions and fatality cases. Up to October 4, 2023, there are a total of 771,151,224 confirmed COVID-19 cases, including 6,960,783 death cases [1]. India is also struggling with this pandemic with a large number of contagions and fatalities. On October 4, 2023, there have been 44,998,838 COVID-19confirmed cases reported in India, including 532,032 fatality cases. To control the COVID-19 contagions, scientists, researchers, and medical professionals constantly searching for effective vaccines, preventative measures, and strategies for better treatment. Due to numerous COVID-19 variants, scientists are striving to develop a more effective vaccine to reduce contagion. It is predicted that the immunization programme will avert between 2–3 million fatalities annually [2]. The impact of different COVID-19 vaccines in reducing the spread of the disease can be discussed in [3]. The effectiveness of COVID-19 vaccines

E-mail address: avenkateshmaths@gmail.com (A. Venkatesh).

https://doi.org/10.1016/j.rico.2023.100345

^{*} Corresponding author.

has been shown to be up to 95% in reducing symptomatic COVID-19 contagions. According to the literature, numerous research articles with various perspectives have recently been created and published in related to minimizing this COVID contagion.

The mathematical modeling of contagious diseases is a significant tool for the analysis of transmission dynamics of contagious disease, to predict the trajectory of an epidemic and to evaluate best strategies to control an epidemic. It can also provide useful insights concerning transmission patterns and detection of biological parameters that influence the disease spread and most effective control strategies. To comprehend the dissemination dynamics of COVID-19 pandemic, numerous mathematical models are proposed [4–6]. Shirouyehzad et al. [7] conducted an assessment of the effectiveness of countries impacted by the COVID-19 pandemic, employing Data Envelopment Analysis(DEA) to examine the influence of population density and health system infrastructures. Radha et al. [8,9] examined the properties of pentapartitioned neutrosophic (PN) sets and interval-valued pentapartitioned neutrosophic sets (IVPN) while focusing on the enhancement of correlation coefficients. Mujahid et al. [10] conducted a decision-making analysis aimed at lowering the mortality rate associated with the COVID-19 pandemic. They employed the q-rung orthopair fuzzy soft Bonferroni mean operator as a computational tool for their investigation. Mohsen et al. [11] developed a numerical methodology to analyze a distributed order time fractional model of the COVID-19 contagion. The finite difference scheme and the midpoint quadrature approach are utilized to solve this problem. Momena et al. [12] focused on the identification of illness symptoms, followed by the application of a Multi-Criteria Decision Making (MCDM) diagnosis approach to identify the probable ailment. For modeling and forecasting of COVID-19 contagion, Imo et al. [13] developed a novel hybrid intelligent methodology for the optimization of parameter tuning in Interval Type-2 Intuitionistic Fuzzy Logic Systems (IT2IFLS).

In order to effectively mitigate the supply chain disruptions caused by the pandemic in Bangladesh, Doulotuzzaman et al. [14] proposed a number of potential strategies, including contactless delivery, e-commerce adoption, robust collaborative demand forecasting, decentralization of food manufacture and production, and effective information sharing. Imo et al. [15] created a time series analysis of COVID-19 utilizing intuitionistic fuzzy logic, which enables in reluctance and provides membership and non-membership functions which are optimized to forecast COVID-19 contagion cases. Singh et al. [16] constructed a mathematical model to examine the transmission of malaria in individuals with severe infections, considering both crisp and fuzzy environments. Alamin et al. [17] examined the resolution of the dissemination of contagious diseases using the SI model within a fuzzy environment. In [18], Mobasshira investigated the effects of the pandemic on household expenditure in the United States. Specifically, it use analysis of variance (ANOVA) to compare household expenses over two distinct periods. Erinle et al. [19] developed a deterministic model to analyze the dynamic dissemination of the Lassa fever virus including relapse and reinfection rates. Idowu et al. [20] introduced SQEIRVS model and provide empirical evidence supporting a positive association between an increase in transmission rates and the contact with surfaces polluted by droplets from individuals infected with COVID-19. Joshua et al. [21] introduced an innovative and viable human-bat (host-vector) model to predict the transmission and impact of the Ebola virus from bats to humans. Erinle et al. [22] formulated a mathematical model to investigate the transmission dynamics and effect of control strategies bed nets and treatment for malaria infection. Idowu & Loyinmi [23] created a SEQIHRV model to examine the dissemination dynamics of COVID-19 illness and evaluate the influence of control measures as time-dependent measures on the spread of the COVID-19. Soyoung Kim et al. [24] developed an optimal control model to mitigate the spread of influenza. Based on the government's intervention strategies, the simulation period is divided into three subsequent phases. In Period 2, the non-pharmaceutical and antiviral techniques implemented, and in Period 3, the vaccine strategy added.

Mandal et al. [25] developed an epidemic model incorporates quarantine measures and government intervention strategies in order to mitigate the dissemination of COVID-19 disease. Venkatesh and Ankamma Rao [26] formulated the SEAIQHRDP model by using nonpharmaceutical interventions as control strategies to minimize the spread of the COVID disease. Libotto et al. [27] introduced two optimum control problems namely mono-objective multi-objective to evaluate strategy for vaccine in the COVID-19 pandemic. Tchuenche et al. [28] created a an optimal control model with three controls vaccine effectiveness, vaccine waning, and treatment. They also performed a sensitivity analysis on the model. The Khachanji et al. [29] formulated a compartmental model that categorized contagion into nine steps and applied intervention strategies to mitigate the COVID-19 spread. Deng and Zang [30] devised an epidemiological model to evaluate the magnitude of the pandemic and investigate potential control measures, such as the utilization of media campaigns in conjunction with home isolation and the adoption of face-mask wearing strategy to limit the recurrence of the epidemic in Brazil. Alemzewde et al. [31] proposed a deterministic model to evaluate the effectiveness of two therapeutic interventions vaccination and treatment for controlling the COVID-19 pandemic. Venkatesh et al. [32] created a multistrain epidemic model consisting of sixteen compartments to minimize the dissemination of COVID-19 by utilizing vaccine and treatment measures. In this study the cost effective analysis method is applied to determine the best control strategy. For the dynamics of COVID-19 in Ethiopia, Temesgen and Hana [33] constructed the optimal control problem, incorporating three controls namely personal protection, vaccine, and treatment. This study employed a cost-effectiveness analysis to determine the optimum and inexpensive. Acune et al. [34] proposed an optimum control problem that incorporates mixed constraints to analyze various vaccine profiles and determine the most effective vaccination policies for COVID-19. Bishal et al. [35] constructed a optimal control model that integrates age-specific dissemination dynamics of COVID-19 and evaluate the impact of vaccination and treatment strategies on mitigating the burden of COVID-19.

Motivated by the above study, we developed a novel deterministic model consisting of ten compartments to analyze and control the dissemination dynamics of COVID-19 in India. In this study, the individuals who received vaccinations are categorized into three distinct groups: (1) individuals who have received vaccination but remain susceptible to contagion, (2) individuals who have received vaccination with ineffective efficacy and (3) individuals who have received vaccination and are effectively protected from the contagion. Moreover this model extends onto optimal control model to examine the impact of optimal vaccination and treatment

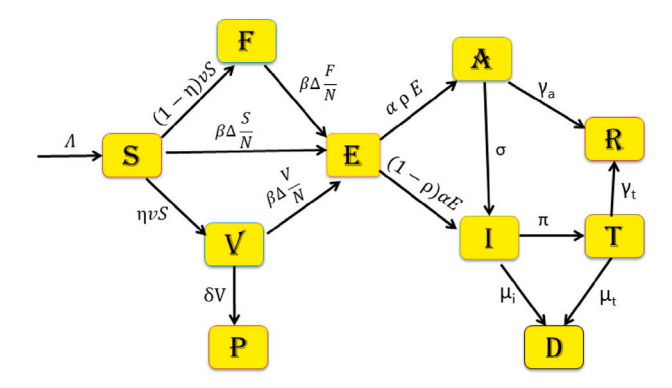


Fig. 1. Flowchart of SVFPEAITRD model.

strategies in mitigating COVID-19 contagions and disease induced mortality. Finally the optimal Vaccination Strategy under varying levels of vaccine efficacy and different vaccination coverages are also evaluated.

The rest of the article is structured as follows. In Section 2, the assumption and formulation of mathematical model is described. In Section 3, the qualitative properties of proposed model are performed. In Section 4, parameters are estimated and sensitivity analysis of R_0 is discussed. In Section 5, the assumption and formulation of the optimal control model are briefly explained. The single and double control strategies are conducted and also vaccination efficacy levels is examined. In Section 6, cost effectiveness analysis is performed to determine the effective control strategy. Finally Section 7 concludes with summary of the results.

2. Model formulation

In this study, the entire population (N) is partitioned into ten distinct groups: susceptible population (S), exposed population (E), effectively vaccinated but still unprotected population (V), ineffectively vaccinated population (F), protected population (P), asymptomatic infected population (I), symptomatic infected population (A), hospitalized population (T), recovered population (R), and deceased population (D). Thus

$$N(t) = S(t) + V(t) + F(t) + P(t) + A(t) + I(t) + T(t) + R(t) + D(t)$$

Compartment S(t) represents the number of individuals who are susceptible to a particular condition or disease. This compartment S is growing by recruitment rate A and decreasing by the natural mortality rate μ . Compartment S reduces by the amount of $\beta \zeta_a A \frac{S}{N}$, which denotes the number of individuals who contracted the virus through interaction with asymptomatic infected individuals, decreases by a factor of $\beta \zeta_a I \frac{S}{N}$, which represents the amount of individuals who have contracted the virus through contact with symptomatic infected individuals and declines by a factor of $\beta \zeta_a T \frac{S}{N}$, which depicting the number of individuals who have contracted the virus through contact with infected individuals who are currently hospitalized. Additionally this compartment S falls by the individuals who have received vaccination at a rate v. Hence, the rate of change of susceptible population per unit time is given by

$$\frac{dS}{dt} = \Lambda - \beta(\zeta_a A + \zeta_i I + \zeta_t T) \frac{S}{N} - (\nu + \mu) S$$

Compartment V(t) depicts the number of individuals who received vaccination effectively yet remain susceptible to contagion. A fully vaccinated individuals might not be totally protected against reinfection and might instead become susceptible to being infected again. The compartment V decreases by the quantity of $\beta \zeta_a A \frac{V}{N}$, which indicating the number of vaccinated persons who got the virus by contact with the asymptomatic individuals, falls by the amount of $\beta \zeta_i I \frac{V}{N}$, which illustrates the number of vaccinated individuals who acquired the virus through interaction with the symptomatic infected individuals and diminishes by the amount of $\beta \zeta_i I \frac{V}{N}$, which represents the number of vaccinated individuals who contracted the virus through contacting with the infected individuals in hospital. This compartment V increases by the amount of $\eta v S$, which shows that the number of susceptible individuals who received perfected vaccination and secured. This compartment V decreases by the rate δ at which the vaccinated individuals are protected and also declines by natural death rate μ . Thus the rate of change of vaccinated population per unit time is represented by

$$\frac{dV}{dt} = -\beta(\zeta_a A + \zeta_i I + \zeta_t T) \frac{V}{N} + \eta v S - (\delta + \mu)V$$

Compartment F(t) shows the number of individuals who received vaccination ineffectively. The compartment F experiences a decrease in value equal to the quantity of $\beta \zeta_a A \frac{F}{N}$. This quantity represents the number of vaccinated individuals who are ineffective in preventing the virus and got it through contact with asymptomatic individuals. Additionally, this compartment F decreases by the amount of $\beta \zeta_t I \frac{V}{N}$, which illustrates the number of ineffective vaccinated individuals who acquired the virus through interaction with symptomatic infected individuals. Furthermore, the compartment F diminishes by the amount of $\beta \zeta_t T \frac{F}{N}$, which demonstrates the number of ineffective vaccinated individuals who contracted the virus through contact with infected individuals admitted to

hospitals. This compartment F also decreases by the amount of $\eta v S$, which denotes the number of susceptible individuals who are perfectly vaccinated and secured. The compartment F grows at a rate of v for those who have received vaccinations and falls at a rate of μ for those who have died naturally. Therefore the rate of change of ineffectively vaccinated population per unit time is described by

$$\frac{dF}{dt} = -\beta(\zeta_a A + \zeta_i I + \zeta_t T) \frac{F}{N} + (1 - \eta) v S - \mu F$$

Compartment P(t) displays the quantity of individuals who have been protected as a result of getting a vaccination. The size of this compartment P grows by the number of vaccinated individuals who are protected at a rate δ , while it is diminished by the natural death rate μ . The rate change of protected individuals per unit time is represented by

$$\frac{dP}{dt} = \delta V - \mu P$$

Compartment E(t) depicts the number of individuals who have been exposed to COVID-19 but have not yet exhibited clinical symptoms. As a result of the susceptible, effectively vaccinated, and ineffectively vaccinated individuals who contracted the virus through contact with asymptomatic infected individuals, symptomatic infected individuals and the individuals who admitted to hospitals due severe contagion, this compartment E grows by the amount of $\beta(\zeta_a A + \zeta_i I + \zeta_i T)(\frac{S}{N} + \frac{V}{N} + \frac{F}{N})$. The decline in this compartment E occurs at a rate of α due to the exposed individuals becomes infected at a rate of α . This compartment E also decreases by the natural mortality rate μ . The rate of change of exposed individuals per unit time is illustrated by

$$\frac{dE}{dt} = \beta(\zeta_a A + \zeta_i I + \zeta_t T)(\frac{S}{N} + \frac{V}{N} + \frac{F}{N}) - (\alpha + \mu)E$$

Compartment A(t) denotes the number of individuals who are infected with a disease but do not exhibit any disease symptoms. Compartment A grows by the amount of $\alpha \rho E$ because a portion ρ of exposed individuals transition to asymptomatic infected (A) at the rate α . This compartment A diminishes by the rate σ because the asymptomatic infected becomes symptomatic infected at the rate σ . This compartment A also reduces by both the recovery rate γ_a of asymptomatic infected individuals and the natural mortality rate μ . The rate of change asymptomatic individuals per unit time is represented by

$$\frac{dA}{dt} = \alpha \rho E - (\sigma + \gamma_a + \mu)A$$

Compartment **I(t)** shows the number of infected individuals who have symptoms of the disease. Given that the remaining portion $(1-\rho)$ of exposed individuals transition to symptomatic infected (I) at a rate of α , the population within this compartment I increases by the quantity $(1-\rho)\alpha E$. The rate π at which infected individuals are admitted to hospitals due to severe contagion produces a reduction in Compartment I. This compartment I also decreases by the rate σ . Furthermore this compartment I reduces by both the mortality rate μ_i of symptomatic infected individuals and the natural mortality rate μ . The rate of change of symptomatic infected individuals per unit time is depicted by

$$\frac{dI}{dt} = (1 - \rho)\alpha E + \sigma A - (\pi + \mu_i + \mu)I$$

Compartment T(t) represents the number of infected individuals who were admitted to the hospital for treatment due to a severe contagion. This compartment T increases by the rate π . The decline in this compartment T occurs by both the mortality rate μ_t of hospitalized individuals and the natural mortality rate μ . The rate of change of hospitalized individuals per unit time is denoted by

$$\frac{dT}{dt} = \pi I - (\gamma_t + \mu_t + \mu)T$$

Compartment R(t) depicts the number of individuals who have successfully recovered from the disease. This compartment R increases by the recovery rates γ_a and γ_t , which correspond to asymptomatic infected individuals and hospitalized patients, respectively. This compartment reduces by the natural mortality rate μ . The rate of change of recovery individuals per unit time is illustrated by

$$\gamma_a A + \gamma_t T - \mu R$$

Compartment D(t) defines the number of individuals who have died as a result of severe contagion. This compartment D rises by the death rate μ_i of symptomatic infected individuals and increases by the mortality rate μ_i of individuals who are hospitalized. The rate of change of deceased individuals per unit time is demonstrated by

$$\frac{dD}{dt} = \mu_i I + \mu_t T$$

A schematic representation of the model is depicted in Fig. 1. The dynamics of the COVID-19 epidemic model are determined by the following system of nonlinear ordinary differential equations:

$$\begin{split} \frac{dS}{dt} &= \Lambda - \beta(\zeta_a A + \zeta_i I + \zeta_t T) \frac{S}{N} - (\nu + \mu) S \\ \frac{dV}{dt} &= -\beta(\zeta_a A + \zeta_i I + \zeta_i T) \frac{V}{N} + \eta \nu S - (\delta + \mu) V \\ \frac{dF}{dt} &= -\beta(\zeta_a A + \zeta_i I + \zeta_i T) \frac{F}{N} + (1 - \eta) \nu S - \mu F \\ \frac{dP}{dt} &= \delta V - \mu P \end{split}$$

Description of all parameters in SVFPEAITRD model.

Parameter	Description	Value	Source
Λ	Human recruitment rate	Varies	_
ζ_a	Modification factor of asymptomatic infected individuals	0.4(0,1)	[36]
ζ_i	Modification factor of symptomatic infected individuals	0.4(0,1)	[37]
ζ,	Modification factor of treatment individuals	0.3(0,1)	[37]
β	Disease transmission rate	0.7571	Estimated
η	vaccine efficacy	0.2814	Estimated
δ	The rate at which vaccinated individuals are protected	0.1673	Estimated
ν	Vaccination rate	0.67	[38]
ρ	Portion of exposed individuals becomes asymptomatic infected	0.3[0.15,0.7]	[39]
α	The rate at which the exposed individuals became infected	0.2[0.071,0.33]	[39]
π	The rate at which symptomatic infected individuals are hospitalized	0.1840	[26]
σ	The rate at which the individuals in asymptomatic infected transition to symptomatic infected	0.0125	[40]
γ_a	Recovery rate of asymptomatic infected individuals	0.034	[40]
γ_t	Recovery rate of hospitalized individuals	0.017	[40]
μ_i	Mortality rate of symptomatic individuals	0.003	[41]
μ_t	Mortality rate of hospitalized individuals	0.0014	[41]
μ	Natural mortality rate	0.0000391	[42]

$$\frac{dE}{dt} = \beta(\zeta_a A + \zeta_i I + \zeta_i T)(\frac{S}{N} + \frac{V}{N} + \frac{F}{N}) - (\alpha + \mu)E$$

$$\frac{dA}{dt} = \alpha \rho E - (\sigma + \gamma_a + \mu)A$$

$$\frac{dI}{dt} = (1 - \rho)\alpha E + \sigma A - (\pi + \mu_i + \mu)I$$

$$\frac{dT}{dt} = \pi I - (\gamma_t + \mu_t + \mu)T$$

$$\frac{dR}{dt} = \gamma_a A + \gamma_t T - \mu R$$

$$\frac{dD}{dt} = \mu_i I + \mu_i T$$
(1)

The primary conditions of the system (1) are taken as $S(0) \ge 0$, $V(0) \ge 0$, $F(0) \ge 0$, $P(0) \ge 0$, $E(0) \ge 0$, $A(0) \ge 0$, $I(0) \ge 0$, $T(0) \ge 0$, $R(0) \ge 0$ and $D(0) \ge 0$.

Table 1 provides the explanation of all model parameters.

3. SVFPEAITRD model analysis

3.1. Positivity and boundedness of the solutions

Theorem 1. All the solutions of the system (1) with primary conditions remain positive and uniformly bounded in the region $\Phi = \{ (S, V, F, P, E, A, I, T, R, D) \in \mathbb{R}^{10}_+ : 0 \le (S + V + F + P + E + A + I + T + R + D) \le \frac{\Lambda}{\mu} \}$

Proof. Let $(S(t), V(t), F(t), P(t), E(t), A(t), I(t), T(t), R(t), D(t)) \in \mathbb{R}^{10}_{+}$ be solution of (1) for $t \in [0, t_0]$ From the first equation of system (1), we have

$$\frac{dS}{dt} = \Lambda - \beta(\zeta_a A + \zeta_i I + \zeta_t T) \frac{S}{N} - (\nu + \mu)S = \Lambda - \Psi S$$

where
$$\Psi(t) = \beta(\zeta_a A + \zeta_i I + \zeta_l T) \frac{1}{N} + (\nu + \mu)$$

Then $\frac{dS}{dt} + \Psi S = \Lambda \geq 0$
After integration, we get

Then
$$\frac{dS}{dt} + \Psi S = \Lambda \ge 0$$

$$S(t) = S_0 \exp\left(-\int_0^t \Psi(s) \, ds\right) + \Lambda \exp\left(-\int_0^t \Psi(s) \, ds\right) \int_0^t e^{\int_0^s \Psi(u) \, du} \, ds > 0$$

The second equation of system (1) gives

$$\frac{dV}{dt} = -\beta(\zeta_a A + \zeta_i I + \zeta_t T) \frac{V}{N} + \eta v S - (\delta + \mu) V \ge -\Phi V$$

where
$$\Phi(t) = (\zeta_a A + \zeta_i I + \zeta_t T) \frac{1}{N} + (\delta + \mu)$$

Then
$$\frac{dV}{dt} \ge -\Phi V$$

By integrating, we get

$$V(t) \ge V(0) \exp\left(-\int_0^t \Phi(u) du\right) \ge 0$$

From the third equation of system (1), we obtain

$$\frac{dF}{dt} = -\beta(\zeta_a A + \zeta_i I + \zeta_t T) \frac{F}{N} + (1-\eta) v S - \mu F \geq -\chi F$$

where $\chi = \beta(\zeta_a A + \zeta_i I + \zeta_t T) \frac{1}{N} + \mu$ Following the integration, we get

$$F(t) \ge F(0) \exp\left(-\int_0^t \chi(u) du\right) \ge 0$$

The fourth equation of system (1) provides

$$\frac{dP}{dt} = \delta V - \mu P \ge -\mu P$$

After the integration process, we obtain

$$P(t) \ge P(0) \exp\left(-\int_0^t \mu \, du\right) \ge 0$$

From the fifth equation of system (1), we get

$$\frac{dE}{dt} = \beta(\zeta_a A + \zeta_t I + \zeta_t T)(\frac{S}{N} + \frac{V}{N} + \frac{F}{N}) - (\alpha + \mu)E \ge -(\alpha + \mu)E$$

By integrating, we obtain

$$E(t) \ge E(0) \exp\left(-\int_0^t (\alpha + \mu) du\right) \ge 0$$

Through the sixth equation of system (1), we have

$$\frac{dA}{dt} = \alpha \rho E - (\sigma + \gamma_a + \mu)A \ge -(\sigma + \gamma_a + \mu)A$$

After the integration, we gain

$$A(t) \ge A(0) \exp\left(-\int_0^t (\sigma + \gamma_a + \mu) du\right) \ge 0$$

Similarly we prove that $I(t) \ge 0$, $T(t) \ge 0$, $R(t) \ge 0$ and $D(t) \ge 0$ Consider the total population

N(t) = S(t) + V(t) + F(t) + P(t) + E(t) + A(t) + I(t) + T(t) + R(t) + D(t)

By adding all equations of system (1) and using above formula, we get

$$\frac{dN}{dt} = \Lambda - \mu N$$

Following the integration, we have

$$N(t) = \frac{\Lambda}{u}(1 - e^{-\mu t}) + N(0)e^{-\mu t}$$
 for $t \ge 0$

If $N(0) \le \frac{\Lambda}{\mu}$ then $N(t) \le \frac{\Lambda}{\mu}$ If $N(0) \ge \frac{\Lambda}{\mu}$, then N(t) asymptotically approaches to $\frac{\Lambda}{\mu}$ and the number of infected population approach to zero for larger t. Hence, all the solution trajectories initiating in \mathbb{R}^{1}_{+} will enter in Φ with finite time.

Therefore Φ is an attracting set. \square

3.2. Contagion-free equilibrium and fundamental reproduction number

Finding an equilibrium points of differential equation is always the first phase in understanding it. In epidemiology there are two different types of equilibrium points. the contagion-free equilibrium point, where the infected population is zero and the endemic equilibrium point at which infection population does not vanish. The local stability of contagion-free and endemic equilibria indicates that these states can be persisted in minor perturbations whereas global stability implies that these states can persist even in the presence of significant perturbations. The global stability of the contagion-free equilibrium point signifies the complete eradication of the disease from the system, while the global stability of the endemic equilibrium point indicates the sustained presence of the disease, leading to its endemic disease. In this section, we discuss about the contagion-free equilibrium of proposed model.

The last equation of the system (1) can be omitted because the preceding nine equations are independent of it. The contagion-free equilibrium E^* of the proposed model is obtained by setting the equations of the system (1) to zero and then using E = A = I = T = 0 to solve the resulting algebraic system for the state variables. Therefore the contagion-free equilibrium is

$$E^* = (\frac{\Lambda}{(\nu+\mu)}, \frac{\Lambda\eta\nu}{(\nu+\mu)(\delta+\mu)}, \frac{\Lambda(1-\eta)\nu}{(\nu+\mu)\mu}, \frac{\Lambda\eta\nu\delta}{\mu(\nu+\mu)(\delta+\mu)}, 0, 0, 0, 0, 0)$$

The fundamental reproduction number R_0 [43–45] is a significant epidemiological factor in discerning the characteristics of a given disease. It measures the dissemination potential of contagious disease in a population. The fundamental reproduction number is defined as the expected number of secondary infected cases that will arise from a single primary infected case in a population that is otherwise susceptible.

When $R_0 < 1$, the existing contagions are less than a single new contagion. In this scenario, the prevalence of the disease will diminish over time and ultimately disappear from existence. If $R_0 = 1$, there exists single contagion only. There will not be an increase in cases or outbreak; the illness will continue to exist in a stable state. When $R_0 > 1$, each contagion that currently exists causes numerous contagions. The transmission of the disease can occur through interaction with others, potentially leading to the emergence of a disease outbreak or epidemic. We find the fundamental reproduction number by using the Next Generation Matrix Method as follows:

$$\mathcal{F} = \begin{pmatrix} -\beta(\zeta_a A + \zeta_i I + \zeta_i T)(S + V + F) \\ 0 \\ 0 \\ 0 \\ 0 \end{pmatrix}$$

$$\mathcal{V} = \begin{pmatrix} (\alpha + \mu)E \\ -\alpha\rho E + (\sigma + \gamma_a + \mu)A \\ -(1 - \rho)\alpha E - \sigma A + (\pi + \mu_i + \mu)I \\ -\pi I + (\gamma_t + \mu_t + \mu)T \end{pmatrix}$$

The Jacobian matrices of two matrices \mathcal{F} and \mathcal{V} are

where $\chi = S + V + F = \frac{\Lambda(\delta + \mu)(\nu + \mu) + \Lambda\nu(\mu - \eta\delta)}{\mu(\delta + \mu)(\nu + \mu)}$

Hence the fundamental reproduction number, the spectral radius of the matrix FV^{-1} is

$$R_0 = \frac{\varLambda(\delta + \mu)(\nu + \mu) + \varLambda\nu(\mu - \eta\delta)}{\mu(\delta + \mu)(\nu + \mu)} \big[\frac{\beta\zeta_a\rho\sigma}{(\alpha + \mu)(\sigma + \gamma_a + \mu)} + \frac{(\beta\zeta_i(\gamma_t + \mu_t + \mu) + (\beta\zeta_t\pi))(\alpha + \rho\sigma) + (\sigma + \gamma_a + \mu)(1 - \sigma)\alpha}{(\alpha + \mu)(\sigma + \gamma_a + \mu)(\pi + \mu_t + \mu)(\gamma_t + \mu_t + \mu)} \big]$$

Theorem 2. When $R_0 < 1$, then the contagion-free equilibrium E^* is locally asymptotically stable and unstable otherwise.

Proof. The Jacobian matrix corresponding to the system (1) at contagion-free equilibrium E^* is

Here $\chi = S^0 + V^0 + F^0 = \frac{A(\delta + \mu)(v + \mu) + Av(\mu - \eta \delta)}{a(\delta + \nu)(v + \mu)}$

The characteristic equation of the matrix J_{E^*} is $|J_{E^*} - \lambda I| = 0$.

$$(\lambda + \mu)^3 (\lambda + (\delta + \mu))(\lambda + (\nu + \mu))$$

$$\begin{vmatrix} -(\alpha+\mu) & \beta\zeta_a\chi & \beta\zeta_i\chi & \beta\zeta_t\chi \\ \alpha\rho & -(\sigma+\gamma_a+\mu) & 0 & 0 \\ (1-\rho)\alpha & \sigma & -(\pi+\mu_i+\mu) & 0 \\ 0 & 0 & \pi & -(\gamma_t+\mu_t+\mu) \end{vmatrix} = 0.$$

$$\Rightarrow (\lambda + \mu)^3 (\lambda + (\delta + \mu))(\lambda + (\nu + \mu))(\lambda^4 + a_1\lambda^3 + a_2\lambda^2 + a_3\lambda + a_4) = 0$$

where

$$\begin{split} a_1 &= (\alpha + \mu) + (\sigma + \gamma_a + \mu) + (\pi + \mu_i + \mu) + (\gamma_t + \mu_t + \mu), \\ a_2 &= ((\alpha + \mu) + (\sigma + \gamma_a + \mu) + (\pi + \mu_i + \mu) + (\gamma_t + \mu_t + \mu))(\gamma_t + \mu_t + \mu) + (\alpha + \mu) \\ &\quad (\sigma + \gamma_a + \mu) + (\sigma + \gamma_a + \mu) + (\pi + \mu_i + \mu)(\gamma_t + \mu_t + \mu) - \chi((1 - \rho)\alpha\beta\zeta_i + \alpha\rho\beta\zeta_a), \\ a_3 &= (\alpha + \mu)[(\sigma + \gamma_a + \mu)(\pi + \mu_i + \mu) + (\sigma + \gamma_a + \mu) + (\pi + \mu_i + \mu)] \\ &\quad + (\sigma + \gamma_a + \mu)(\pi + \mu_i + \mu)(\gamma_t + \mu_t + \mu) - \chi(\pi + \mu_i + \mu)\alpha\rho\zeta_a + (\sigma + \gamma_a + \mu) \\ &\quad (1 - \rho)\alpha\beta\zeta_i + \sigma\alpha\rho\zeta_a + \pi(1 - \rho)\alpha\beta\zeta_i + (\alpha\rho\zeta_a + (1 - \rho)\alpha\beta\zeta_i)(\gamma_t + \mu_t + \mu), \\ a_4 &= (\alpha + \mu)(\sigma + \gamma_a + \mu)(\pi + \mu_i + \mu)(\gamma_t + \mu_t + \mu)(1 - R_0) \end{split}$$

Here $-\mu$, $-\mu$, $(\delta + \mu)$, and $(\nu + \mu)$ are the first five eigen values of J_{E^*} and the remaining four eigen values will be attained from the fourth degree equation $(\lambda^4 + a_1\lambda^3 + a_2\lambda^2 + a_3\lambda + a_4) = 0$

By Routh–Hurwitz criterion, E^* is locally asymptotically stable if $a_1 > 0$, $a_2 > 0$, $a_3 > 0$, $a_4 > 0$ and $a_2a_3a_4 > a_2^2 + a_1a_4^2$

Clearly $a_1 > 0$, $a_2 > 0$, $a_3 > 0$, and $a_4 > 0$ if $R_0 < 1$

It is simple to verify that $a_2a_3a_4 > a_2^2 + a_1a_4^2$ if $R_0 < 1$

Hence the contagion-free equilibrium point E^* is locally asymptotically stable if $R_0 < 1$

Based on Descartes' rule of signs, it can be deduced that there exists at least one positive eigenvalue when $a_4 > 0$ at $R_0 > 1$.

Therefore E^* is locally asymptotically unstable for $R_0 > 1$.

Theorem 3. The contagion free equilibrium $E^* = (\frac{\Lambda}{u}, 0, 0, 0, 0, 0, 0, 0)$ of system (1) is globally asymptotic stable if $R_0 < 1$

Proof. From the system (1), it can be observed that S, V, F, P and R are contagion-free classes, and E, A, I, and T are infected classes. So that (1) can be written as

$$\frac{dX}{dt} = M(X, Y)$$

$$\frac{dY}{dt} = W(X,Y), W(X,0) = 0,$$

where $X = (S, V, F, P, R) \in \mathbb{R}^5_+$ denotes the uninfected population and $Y = (E, A, I, T) \in \mathbb{R}^4_+$ represents the infected populations. Thus $E^* = (X^*, 0)$ identifies the contagion free equilibrium of system (1).

For the system (1), M(X,Y) and W(X,Y) are described as follows:

$$M(X,Y) = \begin{pmatrix} \Lambda - \beta(\zeta_a A + \zeta_i I + \zeta_t T) \frac{S}{N} - (\nu + \mu)S \\ -\beta(\zeta_a A + \zeta_i I + \zeta_t T) \frac{V}{N} + \eta \nu S - (\delta + \mu)V \\ -\beta(\zeta_a A + \zeta_i I + \zeta_t T) \frac{F}{N} + (1 - \eta)\nu S - \mu F \\ \delta V - \mu P \\ \gamma_a A + \gamma_t T - \mu R \end{pmatrix}.$$

$$W(X,Y) = \begin{pmatrix} -\beta(\zeta_a A + \zeta_i I + \zeta_t T)(\frac{S}{N} + \frac{V}{N} + \frac{F}{N}) - (\alpha + \mu)E \\ \alpha \rho E - (\sigma + \gamma_a + \mu)A \\ (1 - \rho)\alpha E + \sigma A - (\pi + \mu_i + \mu)I \\ \pi I - (\gamma_t + \mu_t + \mu)T \end{pmatrix}$$

From the expression M(X, Y), it easily show that M(X, 0) = 0

To prove that E^* is asymptomatically stable globally, the following two conditions shall be satisfied.

- 1. $\frac{dX}{dt} = M(X,0)$ where X^* is asymptotically stable globally.
- 2. $W(X,Y) = KY \overline{W}(X,Y), \ \overline{W}(X,Y) \ge 0, \text{ for } (X,Y) \in \Psi$ where $K = D_Y W(X^*,0)$ is Metzler Matrix

The equations of system (1) can be written as

$$\frac{d}{dt} \begin{pmatrix} S \\ V \\ F \\ P \\ R \end{pmatrix} = M(X,0) = \begin{pmatrix} \Lambda - (\nu + \mu)S \\ \eta \nu S - (\delta + \mu)V \\ (1 - \eta)\nu S - \mu F \\ \delta V - \mu P \\ -\mu R \end{pmatrix}$$

After integrating, we ge

$$S(t) = \frac{\Lambda}{\nu + \mu} + \frac{S(0)}{\nu + \mu} e^{-(\nu + \mu)t},$$

$$V(t) = \frac{\Lambda \eta \nu}{(\nu + \mu)(\delta + \mu)} + \frac{V(0)}{(\nu + \mu)(\delta + \mu)} e^{-(\nu + \mu)(\delta + \mu)t},$$

$$F(t) = \frac{\Lambda(1 - \eta)\nu}{(\nu + \mu)\mu} + \frac{F(0)}{(\nu + \mu)\mu} e^{-(\nu + \mu)\mu t},$$

$$P(t) = \frac{\Lambda \eta \nu \delta}{\mu(\nu + \mu)(\delta + \mu)} + \frac{P(0)}{\mu(\nu + \mu)(\delta + \mu)} e^{-\mu(\nu + \mu)(\delta + \mu)t}$$

$$R(t) = R(0)e^{-\mu t}$$

As $t \to \infty$, we get

S(t) =
$$\frac{\Lambda}{(\nu+\mu)}$$
, $V(t) = \frac{\Lambda\eta\nu}{(\nu+\mu)(\delta+\mu)}$, $F(t) = \frac{\Lambda(1-\eta)\nu}{(\nu+\mu)\mu}$, $P(t) = \frac{\Lambda\eta\nu\delta}{\mu(\nu+\mu)(\delta+\mu)}$ and $R(t) = 0$.
Thus X^* is globally asymptotically stable for $\frac{dX}{dt} = M(X,0)$.

Therefore the first condition is satisfied.

Now the matrices K and $\bar{W}(X,Y)$ of system (1) can be written as K =

$$\left(\begin{array}{ccccc} -(\alpha + \mu) & \beta \zeta_a \chi & \beta \zeta_i \chi & \beta \zeta_t \chi & 0 \\ \alpha \rho & -(\sigma + \gamma_a + \mu) & 0 & 0 & 0 \\ (1 - \rho) \alpha & \sigma & -(\pi + \mu_t + \mu) & 0 & 0 \\ 0 & 0 & \pi & -(\gamma_t + \mu_t + \mu) & 0 \end{array} \right)$$

where
$$\chi = \frac{\Lambda(\delta+\mu)(\nu+\mu) + \Lambda\nu(\mu-\eta\delta)}{\mu(\delta+\mu)(\nu+\mu)}$$

$$\&\, \bar{W}(X,Y) = \begin{pmatrix} \beta \zeta_a A(1-\frac{S}{N}) + \beta \zeta_i I(1-\frac{S}{N}) + \beta \zeta_i T(1-\frac{S}{N}) \\ 0 \\ 0 \\ 0 \\ 0 \end{pmatrix}$$

Since all non-diagonal elements of matrix K is non-negative, K is Metzler matrix and as $S(t) \le N(t)$, $\bar{W}(X,Y) \ge 0$. Thus the second condition also satisfied.

Hence the contagion-free equilibrium E^* is globally asymptotically stable in the region Φ for $R_0 < 1$. \square

4. Numerical simulation

4.1. Model calibration

The method of data fitting involves fitting the proposed model to the collected data and evaluating the fit accuracy. Results are more accurate when a model is well-fitted. We fit the SVFPEAITRD model to the daily confirmed COVID-19 cases in India [46] collected from January 30, 2020 to January 12, 2021 The procedure of fitting the model to COVID-19 data has been executed using the nonlinear least-square function lsqnonlin in MATLAB. By fitting the model to daily confirmed cases, three parameters β , ν and δ are estimated. For simulation the initial values of stated variables are taken as S(0) = 1247185021, V(0) = 0, F(0) = 0, P(0) = 0, E(0) = 6000, A(0) = 10, I(0) = 5, T(0) = 1, R(0) = 1 and D(0) = 0. The values of model parameters are mentioned in Table 1. The Fig. 2 depicts the SVFPEAITRD model fit to COVID-19 data in India. In this Figure, the red solid curve displays the model simulation and the blue dotted curve represents the daily confirmed COVID-19 cases.

4.2. Sensitivity analysis

Sensitivity analysis is a significant tool for examining the importance of various factors in disease dissemination. It aids in understanding of how the reproduction number value varies with respect to various factors. Once these factors are known, a range of techniques can be used to achieve the best results. In [47] presents a thorough investigation of dengue disease sensitivity. The ratio of the relative change in a variable to the relative change in the factor is known as the Normalized forward sensitivity index of the variable with respect to a factor. The sensitivity index can also be constructed using partial derivatives when the variable

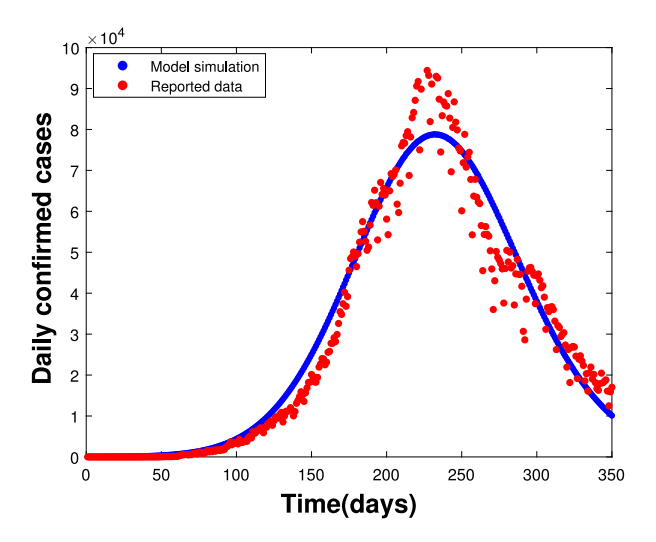


Fig. 2. Model fitting with daily confirmed COVID-19 cases.

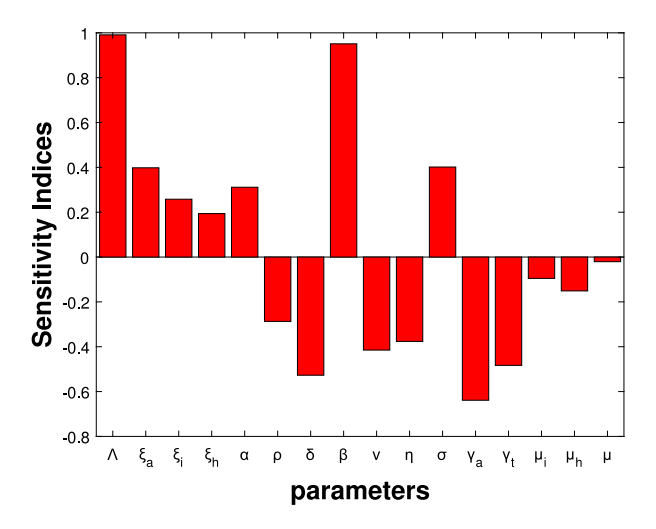


Fig. 3. Sensitivity indices of R_0 with respect to various parameters.

is a function that can be differentiated of the factor. The normalized forward sensitivity index of R_0 , which relies differently on a parameter b, is given by [48], and it is defined as follows:

$$\Gamma_b^{R_0} = \frac{\partial R_0}{\partial b} \frac{b}{R_0}.$$

Fig. 3 depicts the normalized forward sensitivity indices of R_0 . From this Fig. 3, we examined that the parameters Λ , ζ_a , ζ_i , ζ_i , α , β and σ have positive correlations with R_0 as well as the parameters δ , ν , η , γ_a , γ_t , μ_i , μ_t , and μ have negative correlations with R_0 . It is undoubtedly that the three factors protection rate (δ), vaccination rate (ν) and vaccine efficacy (η) have a major impact on the lowering of R_0 . The fundamental reproduction number will also decrease with an increase in treatment rate of hospitalization individuals.

Fig. 4 demonstrates the contour plots of the fundamental reproduction number R_0 with respect to the disease dissemination rate (β) versus vaccination rate (ν) and protection rate (δ) versus vaccination rate (ν) respectively. As shown in Fig. 4(a), R_0 decreases when vaccination rate and protection rate rise. Through increasing the vaccination rate ν , the number of vaccinated individuals increases and the rate of protection is also increases. In Fig. 4(b), it is illustrated that R_0 will rise as disease dissemination rate increases and vaccination rate decreases.

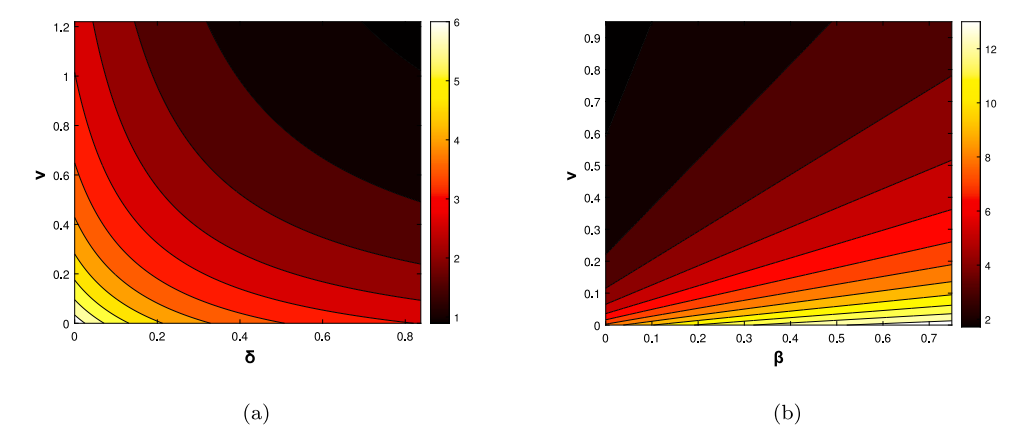


Fig. 4. Contour plots of R_0 as a functions of (a) R_0 versus (δ, ν) (b) R_0 versus (β, ν) .

5. Optimal control

5.1. Optimal control problem

The effective implementation of control measures, such as vaccination or drug therapy, is a significant concern for policymakers, health authorities, and government organizations. Since the substantial financial resources required for the implementation of these control measures, it is crucial to effectively control the dissemination of the disease while simultaneously minimizing overall costs. In this section, we develop an optimum control problem to analyze the impact of optimal vaccine and treatment strategies on minimizing the number of COVID-19 contagions and the total costs associated with the implementation of these control techniques.

Vaccination: Vaccination has been widely recognized as the most effective method for controlling and minimizing the spread of infectious illnesses. Vaccines are administered to the susceptible sub-population in order to activate an immune response that enables the body to identify the pathogen as a potential threat and subsequently eliminate it. This mechanism effectively prevents the propagation of the disease within the susceptible individuals. Vaccination additionally aids in the identification and elimination of any microbes connected with that particular agent, which may be detected in future. The efficacy of COVID-19 vaccines in preventing symptomatic COVID-19 contagions has been demonstrated to be as high as 95%. Therefore the first preventive measure u_1 is the implementation of vaccination. This strategy involves administering vaccines to all susceptible individuals, which results a significant reduction in the propagation of the COVID disease.

Treatment: In order to mitigate the burden of disease and minimize the propagation of contagion, it is crucial to provide better treatment for the infected and hospitalized populations. Based on studies in [49,50], the administration of a combination therapy involving various antiviral drugs (such as Remdesivir, favipiravir, interferon, lopinavir, or arbidol) has the potential to mitigate inflammation in individuals with severe cases of COVID-19. The utilization of a combination therapy involving antiviral medications and immune-modulating drugs is a rational approach, particularly for infected individuals in critical conditions. So that the other two controls u_2 and u_3 are best treatment for the symptomatic infected and hospitalized populations. These treatment would include the administration of immunomodulators like INF or zinc to strengthen the immune system or various prescribed antiviral medications like remdesivir, arbidol, etc. that prevent replication of the virus.

The following optimal control model is created based on above assumptions:

$$\begin{split} \frac{dS}{dt} &= A - \beta(\zeta_a A + \zeta_i I + \zeta_t T) \frac{S}{N} - (u_1 + \mu) S \\ \frac{dV}{dt} &= -\beta(\zeta_a A + \zeta_i I + \zeta_t T) \frac{V}{N} + \eta u_1 S - (\delta + \mu) V \\ \frac{dF}{dt} &= -\beta(\zeta_a A + \zeta_i I + \zeta_t T) \frac{F}{N} + (1 - \eta) u_1 S - \mu F \\ \frac{dE}{dt} &= \beta(\zeta_a A + \zeta_i I + \zeta_t T) (\frac{S}{N} + \frac{V}{N} + \frac{F}{N}) - (\alpha + \mu) E \\ \frac{dP}{dt} &= \delta V - \mu P \\ \frac{dA}{dt} &= \alpha \rho E - (\sigma + \gamma_a + \mu) A \\ \frac{dI}{dt} &= (1 - \rho) \alpha E + \sigma A - (u_2 + \pi + \mu_i + \mu) I \\ \frac{dT}{dt} &= \pi I - (u_3 + \gamma_t + \mu_t + \mu) T \\ \frac{dR}{dt} &= \gamma_a A + \gamma_t T + u_2 I + u_3 T - \mu R \end{split}$$

$$\frac{dD}{dt} = \mu_i I + \mu_t T \tag{2}$$

For the fixed time t_f , the objective functional is defined by

$$J(u_1(t), u_2(t), u_3(t)) = \int_0^{t_f} I + T + \frac{C_1}{2} u_1^2 + \frac{C_2}{2} u_2^2 + \frac{C_3}{2} u_3^2 dt$$
(3)

where C_1 , C_2 and C_3 are weight constants and t_f is final time.

We aim to determine the optimum controls, $u_1(t)$, $u_2(t)$ and $u_3(t)$, such that

$$\mathcal{J}(u_1^*,u_2^*,u_3^*) = \min_{u_1,u_2,u_3 \in U} J(u_1,u_2,u_3),$$

where $U = \{u_1(t), u_2(t), u_3(t): \text{ measurable and } 0 \le u_1(t), u_2(t), u_3(t) \le 1, t \in [0, t_f] \}$

The Pontryagin's Maximum Principle theory [51] provides the necessary requirements that an optimal control system must satisfy.

For our optimal problem, the Hamiltonian \mathcal{H} is given by

$$\mathcal{H} = I + T + \frac{C_1}{2}u_1^2 + \frac{C_2}{2}u_2^2 + \frac{C_3}{2}u_3^2 + \lambda_1 \frac{dS}{dt} + \lambda_2 \frac{dV}{dt} + \lambda_3 \frac{dF}{dt} + \lambda_4 \frac{dP}{dt} + \lambda_5 \frac{dE}{dt} + \lambda_6 \frac{dA}{dt} + \lambda_7 \frac{dI}{dt} + \lambda_8 \frac{dT}{dt} + \lambda_9 \frac{dR}{dt} + \lambda_{10} \frac{dD}{dt}$$

where λ_1 , λ_2 , λ_3 , λ_4 , λ_5 , λ_6 , λ_7 , λ_8 , λ_9 and λ_{10} are the adjoint variables correspond to the state variables S, V, F, P, E, A, I, T, R and D.

Theorem 4. If the couple $(S^*, V^*, F^*, P^*, A^*, I^*, T^*, R^*, D^*)$ is the solution of the control system (2) corresponding to an optimal control u_1^* , u_2^* , u_3^* in U then there exist adjoint variables λ_i that satisfying $\frac{d\lambda_i}{dt} = -\frac{\partial \mathcal{H}}{\partial i}$ with the transversality conditions, $\lambda_i(t_f) = 0$ for i = S, V, F, P, E, A, I, T, R, D. Additionally, for $t \in [0, t_f]$, the optimal controls u_1^* , u_2^* , u_3^* are obtained by $u_1^*(t) = \min\{1, \max\{0, \frac{(\lambda_1 - \lambda_3)S + (\lambda_3 - \lambda_2)\eta S}{C_i}\}\}$,

$$\begin{split} u_1^*(t) &= \min\{1, \max\{0, \frac{(\lambda_1 - \lambda_3)S + (\lambda_3 - \lambda_2)\eta S}{C_1}\}\}, \\ u_2^*(t) &= \min\{1, \max\{0, \frac{(\lambda_7 - \lambda_9)I}{C_2}\}\}, \\ u_3^*(t) &= \min\{1, \max\{0, \frac{(\lambda_8 - \lambda_9)T}{C_2}\}\} \end{split}$$

Proof. The Hamiltonian function is

$$\begin{split} \mathcal{H} &= I + T + \frac{C_1}{2}u_1^2 + \frac{C_2}{2}u_2^2 + \frac{C_3}{2}u_3^2 + \lambda_1(A - \beta(\zeta_a A + \zeta_i I + \zeta_i T)\frac{S}{N} - (u_1 + \mu)) + \lambda_2(-\beta(\zeta_a A + \zeta_i I + \zeta_i T)\frac{V}{N} + \eta u_1 S - (\delta + \mu)) \\ &+ \lambda_3(-\beta(\zeta_a A + \zeta_i I + \zeta_i T)\frac{F}{N} + (1 - \eta)u_1 S) + \lambda_4(\delta V - \mu P) + \lambda_5(-\beta(\zeta_a A + \zeta_i I + \zeta_i T)(\frac{S}{N} + \frac{V}{N} + \frac{F}{N}) - (\alpha + \delta)E) \\ &+ \lambda_6(\alpha \rho E - (\sigma + \gamma_a + \mu)A) + \lambda_7((1 - \rho)\alpha E + \sigma A - (u_2 + \pi + \mu_i + \mu)I) + \lambda_8(\pi I - (u_3 + \gamma_i + \mu_i + \mu)T) \\ &+ \lambda_9(\gamma_a A + \gamma_i T + u_2 I + u_3 T - \mu R) + \lambda_{10}(\mu_i I + \mu_i T) \end{split}$$

Using an adequate partial derivatives of $\mathcal H$ with respect to the state variables, the system of adjoint equations can be derived as

$$\begin{split} \frac{d\lambda_S}{dt} &= -\frac{\partial H}{\partial S} = (\lambda_1 - \lambda_5)\beta(\zeta_a A + \zeta_i I + \zeta_i T) \frac{1}{N} + (\lambda_3 - \lambda_2)\eta u_1 v + (\lambda_1 - \lambda_3)u_1 v + \lambda_1 \mu \\ \frac{d\lambda_V}{dt} &= -\frac{\partial H}{\partial V} = (\lambda_2 - \lambda_5)\beta(\zeta_a A + \zeta_i I + \zeta_i T) \frac{1}{N} + (\lambda_2 - \lambda_4)\delta + \lambda_2 \mu \\ \frac{d\lambda_F}{dt} &= -\frac{\partial H}{\partial F} = (\lambda_3 - \lambda_5)\beta(\zeta_a A + \zeta_i I + \zeta_i T) \frac{1}{N} + \lambda_3 \mu \\ \frac{d\lambda_P}{dt} &= -\frac{\partial H}{\partial P} = \lambda_4 \mu \\ \frac{d\lambda_E}{dt} &= -\frac{\partial H}{\partial E} = (\lambda_7 - \lambda_6)\rho\alpha + (\lambda_5 - \lambda_7)\alpha + \lambda_5 \mu \\ \frac{d\lambda_A}{dt} &= -\frac{\partial H}{\partial A} = -1 + (\lambda_1 - \lambda_5)\beta\zeta_a \frac{S}{N} + (\lambda_2 - \lambda_5)\beta\zeta_a \frac{V}{N} + (\lambda_3 - \lambda_5)\beta\zeta_a \frac{F}{N} + (\lambda_6 - \lambda_7)\sigma \\ &+ (\lambda_6 - \lambda_9)\gamma_a + \lambda_6 \mu \\ \frac{d\lambda_I}{dt} &= -\frac{\partial H}{\partial I} = -1 + (\lambda_1 - \lambda_5)\beta\zeta_i \frac{S}{N} + (\lambda_2 - \lambda_5)\beta\zeta_i \frac{V}{N} + (\lambda_3 - \lambda_5)\beta\zeta_i \frac{F}{N} + (\lambda_7 - \lambda_8)\pi \\ &+ (\lambda_7 - \lambda_9)u_2 + (\lambda_7 - \lambda_{10})\mu_i + \lambda_7 \mu \\ \frac{d\lambda_T}{dt} &= -\frac{\partial H}{\partial T} = -1 + (\lambda_1 - \lambda_5)\beta\zeta_i \frac{S}{N} + (\lambda_2 - \lambda_5)\beta\zeta_i \frac{V}{N} + (\lambda_3 - \lambda_5)\beta\zeta_i \frac{F}{N} \\ &+ (\lambda_7 - \lambda_8)\pi + (\lambda_8 - \lambda_9)u_3 + (\lambda_8 - \lambda_{10})\gamma_i + (\lambda_8 - \lambda_{10})\mu_i + \lambda_8 \mu \\ \frac{d\lambda_R}{dt} &= -\frac{\partial H}{\partial R} = \lambda_9 \mu \\ \frac{d\lambda_D}{dt} &= -\frac{\partial H}{\partial D} = 0 \end{split}$$

By differentiating the Hamiltonian \mathcal{H} with respect to optimum controls u_1 , u_2 , u_3 and using optimum conditions $\frac{\partial \mathcal{H}}{\partial u_1} = 0$, $\frac{\partial \mathcal{H}}{\partial u_2} = 0$, and $\frac{\partial \mathcal{H}}{\partial u_3} = 0$, we get

$$\begin{split} \frac{\partial \mathcal{H}}{\partial u_1} &= C_1 u_1 + \lambda_1 (-S) + \lambda_2 (\eta S) + \lambda_3 (1 - \eta) S \Rightarrow u_1 = \frac{(\lambda_1 - \lambda_3) S + (\lambda_1 - \lambda_2) \eta S}{C_1} \\ \frac{\partial \mathcal{H}}{\partial u_2} &= C_2 u_2 - \lambda_7 I + \lambda_9 I \Rightarrow u_2 = \frac{(\lambda_7 - \lambda_9) I}{C_2} \end{split}$$

$$\frac{\partial \mathcal{H}}{\partial u_3} = C_3 u_3 - \lambda_8 T + \lambda_9 T \Rightarrow u_3 = \frac{(\lambda_8 - \lambda_9) T}{C_3}$$

Hence, for these controls u_1^* , u_2^* , u_3^* , we get optimum values of \mathcal{J}

5.2. Optimal control model simulation

In this section numerical simulation is performed to evaluate the effectiveness of both vaccination and treatment strategies over a period of 300 days. The results are simulated in MATLAB software using a combination of forward and backward difference approximations methods [52]. The extended system (2) is solved by using forward difference approximation, whereas the adjoint state system is solved by employing backward difference approximation.

The parameter values that are listed in Table 1 are used for this simulation. It is assumed that the value of weight constant C_1 is 10^{15} based on the studies in [35,53] and the values of the weight constants C_2 and C_3 are taken as 200 and 100 respectively.

We analyze three different cases in this simulation.

- 1. Optimal vaccination and treatment strategy
- 2. Optimal vaccination strategy under various vaccination coverages
- 3. Optimal vaccination strategy under various vaccine efficacy levels

5.3. Optimal vaccination and treatment strategy

This section analyze the impact of optimal vaccination and treatment strategies in reducing the COVID -19 contagions. Fig. 5 displays the proportions of asymptomatic infected, symptomatic infected, treatment and dead populations under different combinations of optimal controls strategies. This Fig. 5 reveals that the combination of vaccination and treatment strategies is more effective at minimizing COVID-19 contagions and disease-related fatalities than the vaccination strategy or treatment strategy alone. Comparing the vaccine strategy to the treatment strategy, we also observe that the vaccination strategy is more effective at lowering COVID-19 contagions and fatalities. Fig. 6 illustrates the changes in control profile when the cost of different controls decreases. It is observed that a decline in the cost of control parameters leads to an increase in the duration required to maintain these controls at 1. This phenomenon is demonstrated that as the costs associated with vaccines and drugs for implementing these controls decrease, the probability of more investment on these measures would increase.

5.4. Optimal vaccination strategy under various vaccination coverages

In this section, we examine the impact of an optimal vaccination strategy on the COVID-19 contagions at various vaccine coverage levels. The values of weight constant C_1 are taken as 10^{11} , 10^{13} and 10^{15} . In this cases larger value indicates that the cost related to vaccination is high, which results in lower vaccination coverages. Fig. 7 represents the variations in total infected and deceased populations with respect to C_1 . This Fig. 7 illustrates that a decrease in the weight constant value leads to a reduction in the proportions of both infected and deceased populations. This happens due to implementation of more expensive vaccines results in lower vaccination rates, which increases the incidence of contagions and fatalities. Therefore widespread use of vaccines can limit the dissemination of COVID-19 which leads to a reduction in deaths and contagions peaks.

5.5. Optimal vaccination strategy under various vaccine efficacy levels

The efficacy of vaccines may vary over time as new variants with various mutations appear. In this section, we alter the vaccination efficacy levels against COVID-19 disease and evaluate their impact on the proportion of COVID-19 contagions and fatalities. Using three distinct vaccine efficacy levels 60%, 80%, and 90% of the vaccine, we plot the proportions of both infected and dead populations in Fig. 8. This Fig. 8 demonstrates that as vaccine efficacy levels increase, the total number of COVID-19 contagions and fatalities decline. This concludes that the COVID-19 contagions peak can be reduced by the implementation of vaccines with higher efficacy.

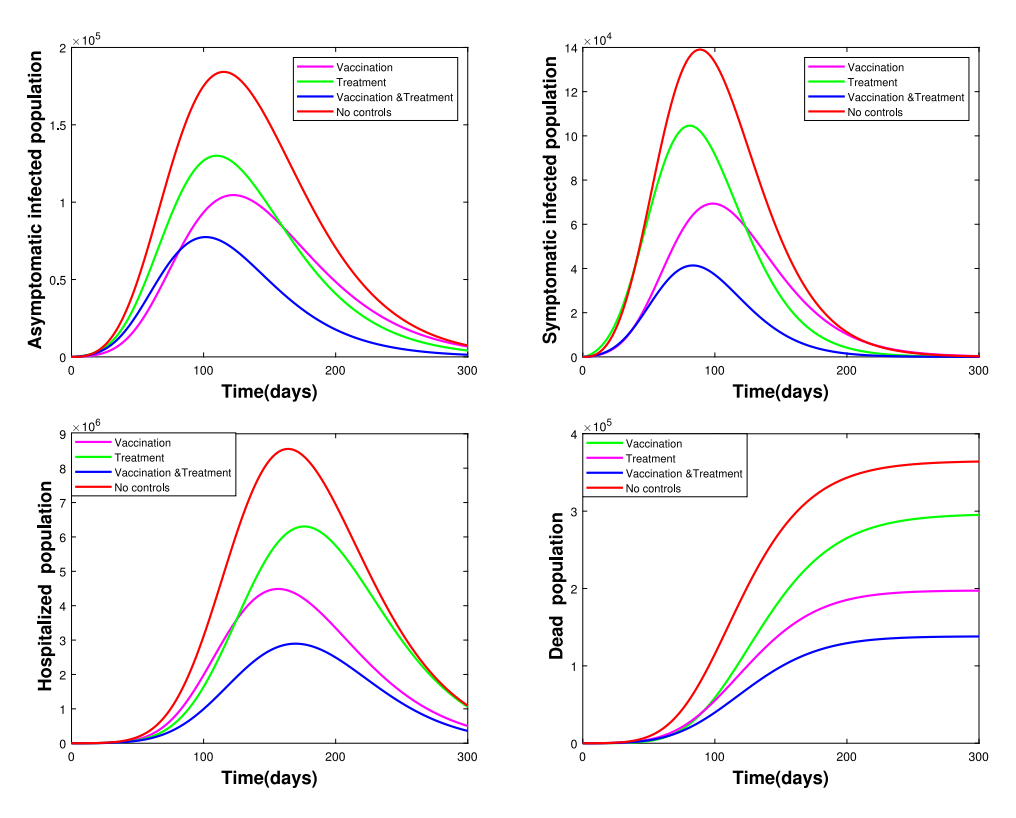


Fig. 5. Variations in asymptomatic infected, symptomatic infected, hospitalized, and dead populations under different optimal control strategies.

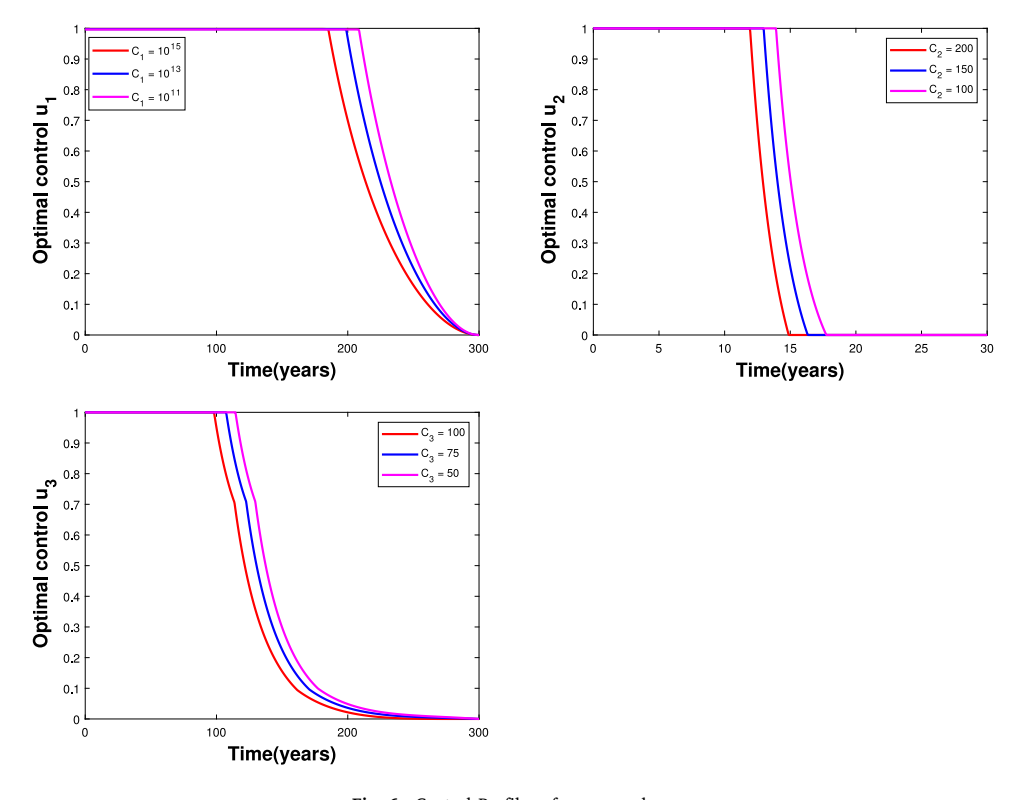


Fig. 6. Control Profiles of u_1 , u_2 , and u_3 .

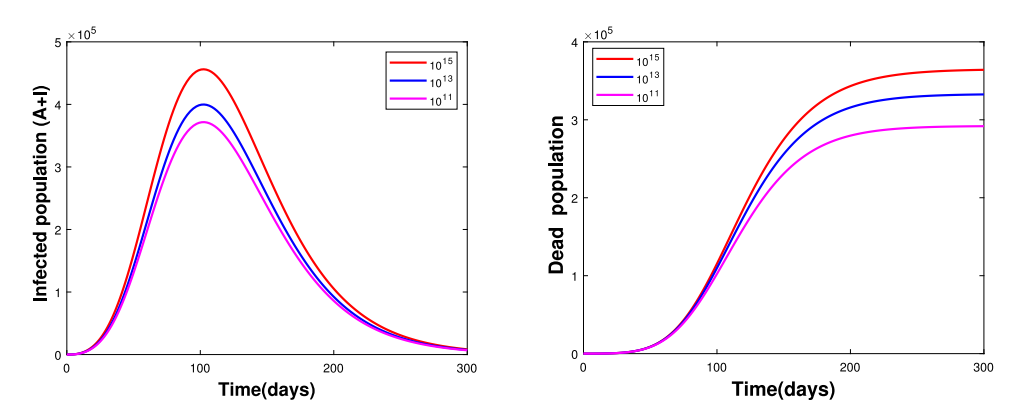


Fig. 7. Under various vaccination Coverages (a) the infected population (A+I) (b) the dead population.

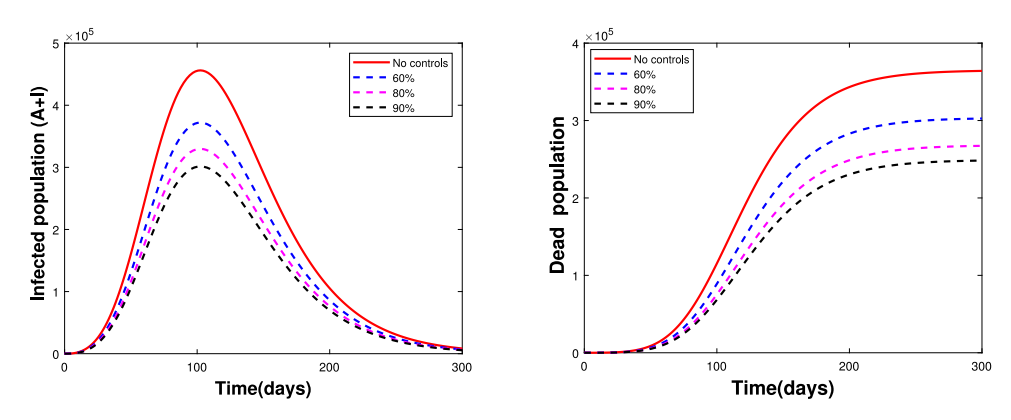


Fig. 8. Under various vaccine efficacy levels (a) the infected population (A+I) (b) the dead population.

6. Cost-effectiveness analysis

In order to effectively minimize the dissemination of COVID-19 at the lowest feasible cost, it is crucial to identify the most cost-effective optimal control strategy among the single and combined control strategies. The cost effectiveness analysis enables the demonstration of the economic advantages related to each control strategy. It is used to compare the relative costs as well as outcomes of various strategies. In this study the cost effectiveness is comprehensively investigated using the incremental cost effectiveness ratio (ICER) [32,54], which evaluates the variances between the costs and health outcomes of the two competing intervention techniques. Let C_V , C_T and C_{VT} represent the vaccination control strategy, treatment control strategy and combination of vaccination and treatment strategy. The ICER is determined by dividing the difference in costs between strategies X and Y by the difference in the number of contagions averted between strategies X and Y where $X, Y \in \{C_T, C_V, C_{VT}\}$.

Given two competing strategies X and Y, where strategy Y is more effective than strategy X (TA(Y) > TA(X)), the ICER values are computed as follows:

$$ICER(X) = \frac{TC(X)}{TA(X)}$$

$$ICER(Y) = \frac{TC(Y) - TC(X)}{TA(Y) - TA(X)}$$

where the total cost (TC) of each strategy is calculated using the objective functional (3) and the total contagions averted (TA) is computed by subtracting the total number of COVID-19 contagions with strategy from the total number of COVID-19 contagions without strategy.

The values of total averted COVID-19 contagions and total costs of control strategies C_V , C_T and C_{VT} is listed in Table 2 in an ascending order of total averted COVID-19 contagions.

Now we compute and compare the strategy C_T with strategy C_{VT} as shown Table 3 The ICER of C_T and C_{VT} are calculated as follows:

$$ICER(C_T) = \frac{5.8 \times 10^4}{3.3 \times 10^6} = 0.0175$$

Table 2
Control strategies in increasing order averted contagions.

Strategy	Total averted contagions (TA)	Total cost (TC)
C_T	3.3×10^6	5.8×10^{4}
C_V	4.1×10^6	7.6×10^4
C_{VT}	6.7×10^6	7.1×10^4

Table 3 Total averted contagions, total costs and ICER values of C_V and C_{VT} .

Strategy	Total averted contagions (TA)	Total cost (TC)	ICER
C_T C_{VT}	3.3×10^6 6.7×10^6	5.8 ×10 ⁴ 7.1 ×10 ⁴	0.0175 0.0038

Table 4 Total averted contagions, total costs and ICER for control strategies C_V and C_{VT} .

Strategy	Total averted contagions (TA)	Total cost (TC)	ICER
C_V	4.1 ×10 ⁶	7.6 ×10 ⁴	0.0185
C_{VT}	6.7×10^6	7.1×10^4	-0.0019

$$ICER(C_{VT}) = \frac{(7.1 - 5.8) \times 10^4}{(6.7 - 3.3) \times 10^6} = 0.0038$$

Comparing C_T to C_{VT} , the ICER of C_T is higher than ICER of C_{VT} . This reveals that C_T is more expensive and less efficient than C_{VT} . Hence the implementation of treatment control strategy C_T removed from the list. The next comparison of strategy C_V with strategy C_{VT} is mentioned in Table 4.

The ICER for \mathcal{C}_V and \mathcal{C}_{VT} are computed as follows:

$$ICER(C_V) = \frac{(7.6) \times 10^4}{(4.1) \times 10^6} = 0.0185$$

$$ICER(C_{VT}) = \frac{(7.1 - 7.6) \times 10^4}{(6.7 - 4.1) \times 10^6} = -0.0019$$

Since ICER of C_{VT} is less than ICER of C_V , strategy C_{VT} is less expensive and more effective than C_V . Hence the implementation of vaccination control strategy C_V is eliminated from the list. In light of this, it can be shown that the combination of vaccination and treatment control strategy is effectively minimizing the COVID-19 contagions and disease induced mortality in the population.

6.1. Limitations

- This study focuses exclusively on the effects of pharmaceutical interventions on COVID-19 infections, and does not encompass non-pharmaceutical interventions such as awareness programs and safety measures.
- This model does not incorporate the stability analysis of the endemic equilibrium of the model due to the presence of ten compartments.

6.2. Future research scope

There will be scope on creating an optimal control model to analyze the dynamics of COVID-19 and TB or HIV/AIDS co-contagion and evaluate the impact of pharmaceutical and non-pharmaceutical interventions on this co-contagion problem.

7. Conclusions

In this study a ten compartment mathematical model was formulated to analyze and mitigate the dissemination of COVID-19 contagion in India. The positivity and boundedness of the model were first established, and then its fundamental reproduction number was determined to be 1.847. The contagion-free equilibrium was both locally and globally asymptotically stable if R_0 is below unity. By fitting the proposed model to the daily confirmed COVID-19 cases in India and estimated the disease transmission rate, vaccine efficacy and protection rate. Sensitive analysis of R_0 was determined that if vaccination rate rises then the vaccine effectiveness, protection rate, and recovery rate increase. As a result, the dissemination of COVID-19 can be controlled. Furthermore the proposed model was extended to an optimal control problem to evaluate the impact of treatment and vaccination strategies on COVID-19 contagions over a 300 days period. Single and combined control strategies were conducted. The numerical analysis shown that each strategy has potential to mitigate the dissemination of COVID disease. Cost-effectiveness analysis was revealed that the combination of vaccination and treatment strategy was most effective and least costly strategy in minimizing the COVID-19

contagions and disease-induced deaths. Finally, it was determined that if vaccine efficacy risen, COVID-19 contagions and disease-related deaths were significantly reduced. The goal of this study is to better understand the role that treatment and vaccination as preventive strategies in reducing COVID-19 contagions, in order to aid policymakers in developing techniques that effectively prevent the further spread of the COVID-19 disease.

Declaration of competing interest

The authors declare that they have no known competing financial interests or personal relationships that could have appeared to influence the work reported in this paper. No specific grant for this research was provided by funding organizations in the public, private, or not-for-profit sectors.

Data availability

The data used for this work is publicly available at https://data.covid19india.org/csv/latest/case time series.csv.

Acknowledgments

We would like to thank Reviewers for taking the time and effort necessary to review the manuscript. We sincerely appreciate all valuable comments and suggestions, which help us to improve the quality of the manuscript.

References

- [1] https://www.worldometers.info/coronavirus. 2020.
- [2] Sari RA, Habibah U, Widodo A. Optimal control on model of SARS disease spread with vaccination and treatment. J Exp Life Sci 2017;7:61-8.
- [3] Agarwal SK, Naha M. COVID-19 vaccine coverage in India: A district-level analysis. Vaccines (Basel) 2023;11(5):948.
- [4] Anggriani N, Ndii MZ, Amelia R, et al. A mathematical COVID-19 model considering asymptomatic and symptomatic classes with waning immunity. Alex Eng J 2022;61:113–24.
- [5] Singh A, Arquam M. Epidemiological modeling for COVID-19 spread in India with the effect of testing. Physica A 2022;592:126774.
- [6] Kifle Zenebe Shiferaw, Obsu Legesse Lemecha. Mathematical modeling for COVID-19 transmission dynamics: A case study in Ethiopia. Results Phys 2022:34:105191.
- [7] Shirouyehzad H, Jouzdani J, Karimvand MK. Fight against COVID-19: A global efficiency evaluation based on contagion control and medical treatment. J Appl Res Ind Eng 2020;7(2):109–20.
- [8] Radha R, Arul Mary A, Broumi S, et al. Chapter 12 Improved correlation coefficients in neutrosophic statistics for COVID patients using pentapartitioned neutrosophic sets. In: Cognitive data science in sustainable computing, Cognitive intelligence with neutrosophic statistics in bioinformatics. 2023, p. 237–58.
- [9] Radha R, Arul Mary A, Broumi S, et al. Chapter 18 Effectiveness on impact of COVID vaccines on correlation coefficients of pentapartitioned neutrosophic pythagorean statistics. In: Smarandache Florentin, Aslam Muhammad, editors. Cognitive data science in sustainable computing. Cognitive intelligence with neutrosophic statistics in bioinformatics. 2023, p. 335–56.
- [10] Abbas M, Asghar MW, Guo Y. Decision-making analysis of minimizing the death rate due to covid-19 by using q-rung orthopair fuzzy soft Bonferroni mean operator. J Fuzzy Ext Appl 2022;3(3):231–48.
- [11] Khasteh M, Refahi Sheikhani AH, Shariffar F. A novel numerical approach for distributed order time fractional COVID-19 virus model. J Appl Res Ind Eng 2022;9(4):442–53.
- [12] Alaa FM, Shubhendu M, Kamal Hossain G, et al. Prediagnosis of disease based on symptoms by generalized dual hesitant hexagonal fuzzy multi-criteria decision-making techniques. MDPI Syst 2023;11(5):1–38.
- [13] Eyoh IJ, Adeoye OS, Inyang UG. Hybrid intelligent parameter tuning approach for COVID-19 time series modeling and prediction. J Fuzzy Ext Appl 2022;3(1):64–80.
- [14] Xames D, Tasnim F, Mim T. COVID-19 and food supply chain disruptions in Bangladesh: Impacts and strategies. Int J Res Ind Eng 2022;11(2):155-64.
- [15] Eyo I, Eyoh J, Umoh U. On the prediction of Covid-19 time series: An intuitionistic fuzzy logic approach. J Fuzzy Ext Appl 2021;2(2):171-90.
- [16] Payal S, Bhumi G, Kamal Hossain G, et al. Analysis and interpretation of Malaria disease model in crisp and fuzzy environment. Results Control Optim 2023;12:100257.
- [17] Alamin A, Sankar Prasad M, Kunal B, et al. Analysis of discrete system modelling followed by spread of infectious diseases problem in fuzzy environments. Math Models Infect Dis Soc Issues 2020;120–37.
- [18] Zaman Mobasshira. Evaluation of household expenditure in the United States: Pre-covid and post-covid statistical analysis. Int J Res Ind Eng 2023. http://dx.doi.org/10.22105/riej.2023.383801.1364.
- [19] Erinle-Ibrahim LM, Adebimpe O, Lawal WO. A mathematical model and sensitivity analysis of Lassa fever with relapse and reinfection rate. Tanzan J Sci 2022;48(2):414–26.
- [20] Kabir Oluwatobi I, Adedapo Chris L. Impact of contaminated surfaces on the transmission dynamics of Corona virus disease (COVID-19). Biomed J Sci & Tech Res 2023;51(1):42280–94.
- [21] Joshua Oluwasegun A, Adedapo Chris L. Modelling the impact of some control strategies on the transmission dynamics of Ebola virus in human-bat population: An optimal control analysis. Heliyon 2022;8(12):e12121.
- [22] Erinle-Ibrahim LM, Idowu OK, Sulola Abigail I. Mathematical modelling of the transmission dynamics of Malaria infection with optimal control. Kathmandu Univ J Sci Eng Technol 2021;15(3):1–8.
- [23] Idowu OK, Loyinmi AC. Qualitative analysis of the transmission dynamics and optimal control of Covid-19. EDUCATUM J Sci Math Technol 2023;10(1):54–70.
- [24] Kim S, Lee J, Jung E. Mathematical model of transmission dynamics and optimal control strategies for 2009 A/H1N1 influenza in the Republic of Korea. J Theoret Biol 2017;412:74–85.
- [25] Mandal M, Jana S, Nandi SK, et al. A model based study on the dynamics of COVID-19: Prediction and control. Chaos Solitons Fractals 2020;136:109889.
- [26] Ankamma Rao M, Venkatesh A. SEAIQHRDP mathematical model analysis for the transmission dynamics of COVID-19 in India. J Comput Anal Appl 2023;31:96–116.
- [27] Libotte GB, Lobato FS, Platt GM, et al. Determination of an optimal control strategy for vaccine administration in COVID-19 pandemic treatment. Comput Methods Programs Biomed 2020:196:105664.

- [28] Tchuenche JM, Khamis SA, Agusto FB, et al. Optimal control and sensitivity analysis of an Influenza model with treatment and vaccination. Acta Biotheor 2010;59:1–28.
- [29] Khajanchi S, Sarkar K, Banerjee S. Modeling the dynamics of COVID-19 pandemic with implementation of intervention strategies. Eur Phys J Plus 2022;137.
- [30] Deng Y, Zhao Y. Mathematical modeling for COVID-19 with focus on intervention strategies and cost-effectiveness analysis. Nonlinear Dynam 2022;110:3893–919.
- [31] Ayalew Alemzewde, et al. Mathematical model and analysis on the impacts of vaccination and treatment in the control of the COVID-19 pandemic with optimal control. J Appl Math 2023;1–15, edited by Anum Shafiq, 2023, Hindawi Limited, Mar.
- [32] Venkatesh A, Ankamma Rao M, Vamsi DKK. A comprehensive study of optimal control model simulation for COVID-19 infection with respect to multiple variants. Commun Math Biol Neurosci 2023;75:1–33.
- [33] Keno Temesgen Duressa, Etana Hana Tariku. Optimal control strategies of COVID-19 dynamics model. J Math 2023;2050684:1-20.
- [34] Acuña-Zegarra MA, Díaz-Infante S, Baca-Carrasco D, et al. COVID-19 optimal vaccination policies: A modeling study on efficacy, natural and vaccine-induced immunity responses. Math Biosci 2021;337:108614.
- [35] Chhetri B, Vamsi DKK, Prakash DB, et al. Age structured mathematical modeling studies on COVID-19 with respect to combined vaccination and medical treatment strategies. Comput Math Biophys 2022;10:281–303.
- [36] Das P, Shahid Nadim sk, Samhita D. Dynamics of COVID-19 transmission with comorbidity: A data driven modelling based approach. Nonlinear Dynam 2021;106(2):1197–211.
- [37] Mondal J, Khajanchi S. Mathematical modeling and optimal intervention strategies of the COVID-19 outbreak. Nonlinear Dynam 2022;109:177-202.
- [38] https://ycharts.com/indicators/india_coronavirus_full_vaccination_rate.
- [39] Bandekar SR, Ghosh M. Mathematical modeling of COVID-19 in India and its states with optimal control. Model Earth Syst Environ 2021;8(2):2019-34.
- [40] Ghosh SK, Ghosh S. A mathematical model for COVID-19 considering waning immunity, vaccination and control measures. Sci Rep 2023;13.
- [41] Rai RK, Khajanchi S, Tiwari PK, et al. Impact of social media advertisements on the transmission dynamics of COVID-19 pandemic in India. J Appl Math Comput 2021;68:19–44.
- [42] Central Intelligence Agency: India-The World Factbook-CIA. https://www.cia.gov/the-world-factbook/countries/india/people-and-society.
- [43] van den Driessche P, Watmough J. Reproduction numbers and sub-threshold endemic equilibria for compartmental models of disease transmission. Math Biosci 2002;180:29–48.
- [44] Diekmann O, Heesterbeek J, Metz J. On the definition and the computation of the basic reproduction ratio R₀ in models for infectious diseases in heterogeneous populations. J Math Biol 1990;28:365–82.
- [45] Chowell Gerardo, Brauer Fred. The basic reproduction number of infectious diseases: Computation and estimation using compartmental epidemic models. Math Stat Estim Approaches Epidemiology 2009.
- [46] https://data.covid19india.org/csv/latest/case time series.csv.
- [47] Rodrigues HS, Monteiro MTT, Torres DFM. Sensitivity analysis in a Dengue epidemiological model. Conf Pap Math 2013;2013:1-7.
- [48] Chitnis N, Hyman JM, Cushing JM. Determining important parameters in the spread of Malaria through the sensitivity analysis of a mathematical model. Bull Math Biol 2008;70:1272-96.
- [49] Chen Po-Lin. A review of treatment of coronavirus disease 2019 (COVID-19): Therapeutic repurposing and unmet clinical needs. Front Pharmacol 2020;11, Frontiers Media SA, Nov. 2020.
- [50] Shaffer L. 15 Drugs being tested to treat COVID-19 and how they would work. Nature Med 2020. http://dx.doi.org/10.1038/d41591-020-00019-9.
- [51] Pontryagin LS. Mathematical theory of optimal processes. CRC Press; 1987.
- [52] Lenhart S, Workman JT. Optimal control applied to biological models. CRC Press; 2007.
- [53] Lee S, Golinski M, Chowell G. Modeling optimal age-specific vaccination strategies against pandemic influenza. Bull Math Biol 2011;74:958-80.
- [54] Kouidere A, Balatif O, Rachik M. Cost-effectiveness of a mathematical modeling with optimal control approach of spread of COVID-19 pandemic: A case study in Peru. Chaos Solitons Fractals X 2023;10:100090.